Polymer 51 (2010) 232–239

Contents lists available at ScienceDirect

Polymer

journal homepage: www.elsevier.com/locate/polymer

Frustrated structures of polycaprolactam and poly(*p*-benzamide) in their rod–coil–rod triblock copolymers

Junjun Li [a], Youju Huang [a], Yuanhua Cong [a], Lu Xu [a], Daoliang Wang [a], Zhenfei Hong [a], Liangbin Li [a,b,*], Guoqiang Pan [a]

[a] National Synchrotron Radiation Lab, School of Nuclear Science and Technology, University of Science and Technology of China, Hefei, China
[b] CAS Key Laboratory of Soft Matter Chemistry, Department of Polymer Science and Engineering, University of Science and Technology of China, Hefei, China

ARTICLE INFO

Article history:
Received 7 May 2009
Received in revised form
3 September 2009
Accepted 15 November 2009
Available online 20 November 2009

Keywords:
Triblock copolymer
Frustrated structure
Mesomorphic order

ABSTRACT

A series of rod–coil–rod triblock copolymers were synthesized by two-step polycondensation with polycaprolactam (PA6) as the flexible block and poly(*p*-benzamide) (PBA) as the rod. Proton nuclear magnetic resonance (^{1}H NMR), UV–vis spectrophotometry and differential scanning calorimetric (DSC) were first performed to determine the fundamental molecular structure and thermal property of each polymer. Through wide angle X-ray scattering (WAXS), and Fourier transformation infrared spectroscopy (FT-IR) measurements, frustrated structures of both components were studied. For PA6, a quasi-γ mesomorphic order was found in the transition-region nearby the PBA domain which is more favored with the increase of the PBA content owing to stretching from the PBA rod block and different cross-section areas of the rod and coil chains. On the other hand, the mesomorphic order of PA6 segments imposes stretching and constraint on the PBA blocks, which leads to a reduction of order of PBA block when the volume fraction of rod reaches approximately 45%. α crystals of PA6 can form only in the triblock copolymer with low volume fraction of PBA, which exhibit the Brill transition feature during the heating process though this transition ends prematurely as the melting of crystals.

1. Introduction

Rod–coil block copolymers consisting of alternating rigid and flexible blocks tend to outperform other macromolecular materials especially in fiber material area [1,2]. A convincing example is the Spandex® fiber produced by DuPont containing flexible polyglycol and rigid polyurethane [3]. This synthetic polymer fiber is much stronger than rubber and can be stretched to almost 700% of their original length. In fact, nature produces similar materials such as cocoon and spider silks, which can be super strong fibers with shape memory function [4,5]. Their microstructures consist of small crystalline rigid blocks and soft amorphous blocks.

Inspired by nature, a great of effort has been dedicated to synthesize rod–coil block copolymers [6–8]. The key of outstanding performance lies in various microstructures that appear frequently in block copolymers through microphase separation due to the thermodynamic incompatibility between rod and coil blocks [9–12]. Whereas the phase behavior of rod–coil system is more complex than a generic coil–coil system, which is not only parameterized by volume fraction of each block and the Flory–Huggins interaction parameter but also adjusted by intensive rod–rod interaction and geometric mismatch between straight rod and flexible coil [10,11]. A comprehensive review on the synthesis and phase behavior of model rod–coil block copolymers were reported by Lee et al. [12]. After phase separation, the Gaussian coil chain is greatly stretched even under zero-stress condition owing to the competition between elastic energy and interfacial energy. This can be an effective approach to prepare super strong fiber with extended chain configuration, as the orientation of rod can be easily achieved in practice, which can further induce the orientation of the coil. The stretching and the geometric confinement are well known to influence the phase behavior of the coil [12–15]. For example crystallization of coil is slowed down by a hard or soft confinement, where the orientation of crystal can be tuned by the interfacial energy and the geometric effect [16]. On the other hand, the packing of the rods may also be distorted by the ordering of the coil, though it is a passive action with weak effect.

In this work, we synthesized a series of rod–coil–rod triblock copolymers with polycaprolactam (PA6) as the coil and poly(*p*-benzamide) (PBA) as the rod. A similar system, multi-block copolymers comprised of alternating poly(*p*-phenylen eterephthalamide)

* Corresponding author. University of Science and Technology of China, Jinzhai Road 96, 230026 Hefei, China. Tel.: +86 0551 3602081; fax: +86 0551 5141078.
E-mail address: lbli@ustc.edu.cn (L. Li).

0032-3861/$ – see front matter © 2009 Elsevier Ltd. All rights reserved.
doi:10.1016/j.polymer.2009.11.035

and polyamide 6,6 blocks, has been studied by De Ruijter et al. [17,18]. However, the specific details of coil and rod blocks including their frustrated structure are still unrevealed. The aim of current work is to explore the state of both components within the triblock copolymers, which may influence the properties of material to a large extent.

The morphology of the rod–coil–rod triblock copolymer is mainly determined by three factors: (i) the intensive π–π interactions and hydrogen bond linkages between the flat aromatic polyamide chains; (ii) the lattice mismatch between straight PBA and flexible PA6 blocks, which may induce the appearance of mesomorphic order as suggested by Matheson and Flory [19]; (iii) the crystalline diversity of PA6. Homopolymer PA6 can mainly form two different crystals α and γ at room temperature, which are monoclinic, though other crystalline forms like α′ and γ′ were also reported. A mesophase was obtained upon quenching the molten PA6, though its structural detail is still not fully understood [20–24]. PBA as a wholly aromatic polyamide generally forms an orthorhombic crystal, where the rod-like chains are parallel with each other [25].

In the following section, we first describe the synthesis procedure of the series of rod–coil–rod triblock copolymers, and then investigate the states of both PA6 and PBA blocks. Our results from wide angle X-ray scattering (WAXS), differential scanning calorimetry (DSC) and Fourier transformation infrared spectroscopy (FT-IR) suggest that: (i) a quasi-γ mesomorphic order of PA6 is formed, and the content of which increases along with the volume fraction of PBA; (ii) the crystalline ordering of PBA is constrained when the elastic energy of PA6 caused by microphase separation is large enough.

2. Experimental section

2.1. Materials

1-Methyl-2-pyrrolidone (NMP) and pyridine (Py) were refluxed and distilled over calcium hydride before used. Triphenyl phosphite (TPP) was stored over 4A molecular sieves. Lithium chloride (LiCl) and calcium chloride ($CaCl_2$) were dried at 300 °C for 5 h before used. Hexane diacid, ϵ-caprolactam and *p*-aminobenzoic acid were vacuum dried at 50 °C over 24 h and stored in the desiccator. N, N-dimethylacetamide (DMAc), alcohol, acetone and formic acid (88%) were used as received without any purification. All the reagents were purchased from Sinopharm Chemical Reagent Co., Ltd. (Shanghai, China).

2.2. Synthesis procedure

The series of triblock copolymers were synthesized by two-step polycondensation as shown in Scheme 1. Polycaprolactam (PA6) was chosen as the coil block and poly(*p*-benzamide) as the rod. Here, the molecular mass of PA6 blocks was a constant and the desired rod–coil–rod copolymers were made by varying the feeding ratio of PA6/*p*-aminobenzoic acid.

2.2.1. HOOC–PA6–COOH

In a high-pressure reactor equipped with a mechanical stirrer and two gas inlets, 200 g of ϵ-caprolactam, 8.00 g of hexane diacid and 5.00 mL of water were charged. After vacuumized and injected nitrogen for 5 times, the oxygen-free reactor was complete sealed and heated up to 220 °C gradually. The melt-polycondensation was lasted 10 h and then cooled to room temperature. In this way, carboxyl-terminated PA6 oligomer (HOOC–PA6–COOH) with a certain molecular weight was prepared [24]. In order to remove the cyclic oligomers and other small molecules, the bulk PA6 was dissolved in formic acid, and then poured into a large excess of hot water with vigorous stirring. The resulting products were further purified with hot water for another 5 times and then vacuum dried at 60 °C.

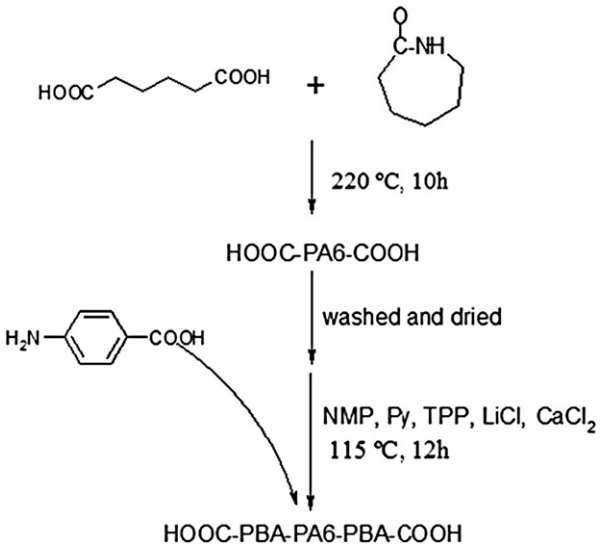

Scheme 1. Synthesis procedure of PBA–PA6–PBA triblock copolymer.

2.2.2. PBA–PA6–PBA

In a three-neck reaction flask equipped with a constant-pressure dropping funnel and magnetic stirrer under a nitrogen atmosphere, 7.63 g of PA6, 5.10 g of LiCl, 15.00 g of $CaCl_2$, 200 mL of NMP, 50 mL of Py, 30 mL of TPP were charged. After all the solid were dissolved at 100 °C, a solution of *p*-aminobenzoic acid (11.09 g) in NMP (50 mL) was added dropwise [26]. The reaction was kept at 115 °C for 12 h, and then cooled to room temperature to obtain a viscous solution. This solution was precipitated into 2000 mL acetone with vigorous stirring. The prepared products were further extracted in a Soxhlet apparatus using acetone for 24 h and alcohol for another 24 h, then vacuum dried at 60 °C. By varying the added quantity of PA6 (30.49 g for T0.15, 22.87 g for T0.2, 15.25 g for T0.3, 11.43 g for T0.4, 9.15 g for T0.5, 7.63 g for T0.6) a series of triblock copolymers of different rod/coil ratios were obtained.

2.3. Measurement

Each sample of triblock copolymers was dissolved easily in the solvent of DMAc containing 1% lithium chloride at room temperature where the homopolymers (PA6 and PBA) rarely dissolved [27]. By this method, most of the homopolymers can be removed. Before measurement, the solutions were precipitated in deionized water, filtered, washed with deionized water and then dried in a vacuum oven at 60 °C. It is inevitable that homo-PBA exists in our samples even after purification by dissolution and precipitation method, because all of them were prepared by polycondensation. Therefore UV–vis spectrophotometry (UV-2802PC, UNICO Instruments) was employed using the method in Ref. [32] to determine the content of homo-PBA through amino groups which is peculiar to homo-PBA (triblock copolymers were terminated by carboxyl groups).

Proton nuclear magnetic resonance (^{1}H NMR) spectra of each copolymer sample in D_2SO_4 were obtained with a 400 MHz Super Conducting NMR Spectrometer (Bruker Avance AV 400).

Differential scanning calorimetric (DSC) measurements were performed with a Mettler-Toledo C10358 using a heating rate of 20 °C/min.

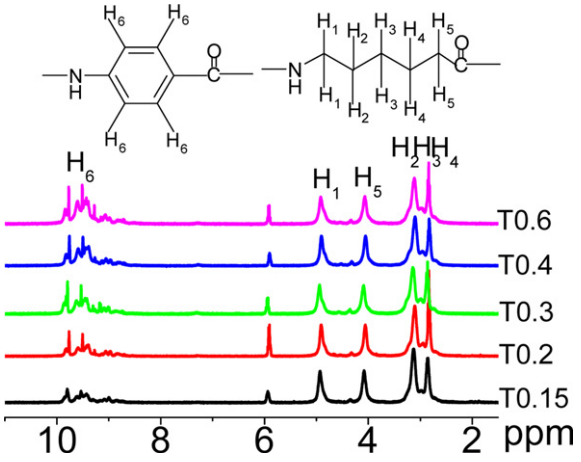

Fig. 1. ^{1}H NMR spectra and the peak assignments of PA6 and PBA in the copolymers.

Wide angle X-ray diffraction (WAXD) measurements were performed at National Synchrotron Radiation Laboratory in Hefei with a wavelength of 0.154 nm.

In situ Fourier transform infrared spectra were collected using a Bruker Tensor 37 FT-IR spectrometer equipped with a heating cell. Room temperature Fourier transform infrared spectra were taken using a Bruker Equinox55 FT-IR spectrometer with pressing potassium bromide troche (KBr).

3. Results

3.1. Molecular mass

The number-average molecular weight of the sandwiched coil block was estimated by end group analysis method. The experimental result of the number-average molecular weight (3000 g/mol) was found to be close to the calculated value (3650 g/mol) and the monomer conversion was approximately 82%.

Fig. 1 shows the ^{1}H NMR spectra and peak assignments of all purified block copolymers. By comparing the relative signal intensities of different protons (protons in the PBA: δ range 8–10 ppm, protons in the PA6: δ range 2–5 ppm), the compositions of copolymers were obtained [17]. UV–vis spectrophotometry results reveal the different content of homo-PBA in each sample. The corresponding results including length of the rod segment in two ends (L_{rod}) [25,28], number-average molecular weight (M_n), volume fraction of PBA (φ_{PBA}) and content of homo-PBA of each sample are shown in Table 1. There is small amount of residual homo-PBA in T0.15, T0.2 and T0.3, but much more in T0.4 and T0.6.

3.2. DSC

Fig. 2 shows the DSC traces (first heating) in the melting region of the copolymers and the pure PA6 we synthesized with a heating rate of 20 °C/min from 0 to 300 °C. The endothermic peaks appear in sample T0.15 and sample T0.2 corresponding to the melting of the PA6 crystals. It is clear that the crystallization of PA6 was suppressed dramatically by the PBA block and the melting points ($T_m \approx 172$ °C for T0.15 and T0.2) were significantly reduced comparing to the melting point of pure PA6 we synthesized ($T_m \approx 217$ °C).

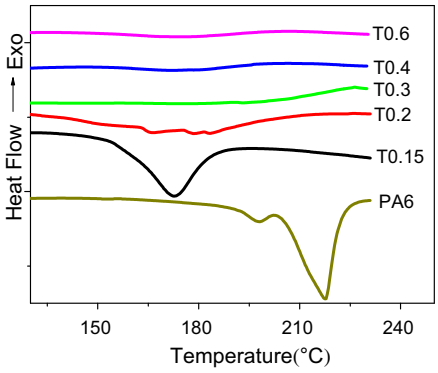

Fig. 2. DSC traces (first heating) in the melting region of the copolymers and the pure PA6 we synthesized (heating rate 20 °C/min).

3.3. WAXD

For the purpose of obtaining better-developed crystalline structure of PBA, all samples were annealed at 180 °C for 2 h and then cooled freely under vacuum condition. Wide angle X-ray diffraction (WAXD) was then performed with a step scanning of temperature (30 °C–300 °C–30 °C, a step of 30 °C, 10 min for every point). For the convenience of comparison, the diffraction peaks of pure PA6 and PBA are summarized in Table 2, respectively [25,28,29].

Fig. 3a, b and d, e shows the WAXD intensity curves of T0.15 and T0.6 (the samples with the lowest and the highest φ_{PBA}) during step heating and cooling scan, respectively. For the convenience to describe, the diffraction peaks at approximately 20° (2θ) are denoted as I, and the peaks at approximately 23° (2θ) are denoted as II. The corresponding *d*-spacing of these two peaks during heating and cooling scan is plotted in Fig. 3c and f for T0.15 and T0.6, respectively. It is very likely that both peaks I and II were caused by overlapping of diffraction peaks of PA6 and PBA. The peak I here is attributed to the diffractions of $(200)_\alpha$ of PA6 and (110) of PBA, and the peak II is the diffractions of $(002)_\alpha/(202)_\alpha$ of PA6 and (200) of PBA. No diffraction peak of γ phase of PA6 is observed in the WAXD curves of all samples. The absence of γ phase is also confirmed by that no obvious change around the diffraction peak positions of γ phase in WAXS curves during the heating and cooling scan. As shown in Fig. 3a and b, during the heating process of T0.15 the intensities of both peaks decrease, while another broad peak arises around 19° (2θ) and retains after the cooling process. This

Table 1
Length of the rod segment in the triblock copolymers (L_{rod}), number-average molecular weight (M_n), volume fraction of PBA (φ_{PBA}) and content of homo-PBA of each sample. The former three were calculated from the ^{1}H NMR spectra, and the last term was analyzed through UV–vis spectrophotometry.

	L_{rod} (nm)	M_n (g/mol)	φ_{PBA} ($\rho_{PBA} = 1.48$ g/cm^3, $\rho_{PA6} = 1.13$ g/cm^3 [27])	Content of homo-PBA (mol/kg)
T0.15	4.34	4605	29.0%	0.0066
T0.2	5.17	4913	32.7%	0.0040
T0.3	7.96	5943	42.8%	0.024
T0.4	9.51	6518	47.2%	0.078
T0.6	11.99	7436	53.0%	0.044

Table 2
The X-ray diffraction peak positions of pure PA6 and PBA. The data marked with * are obtained from the WAXD curve of PA6 ($M_n = 3000$ g/mol) at 30 °C.

hkl	PA6				PBA	
	200 (α)	002 (α)/202 (α)	001 (γ)	200 (γ)	110	200
Interplanar distance (nm)	0.44	0.37/0.36	0.41	0.40	0.44	0.38
2θ (degree)	20.18*	24.21*	21.38	22.20	20.30	23.51

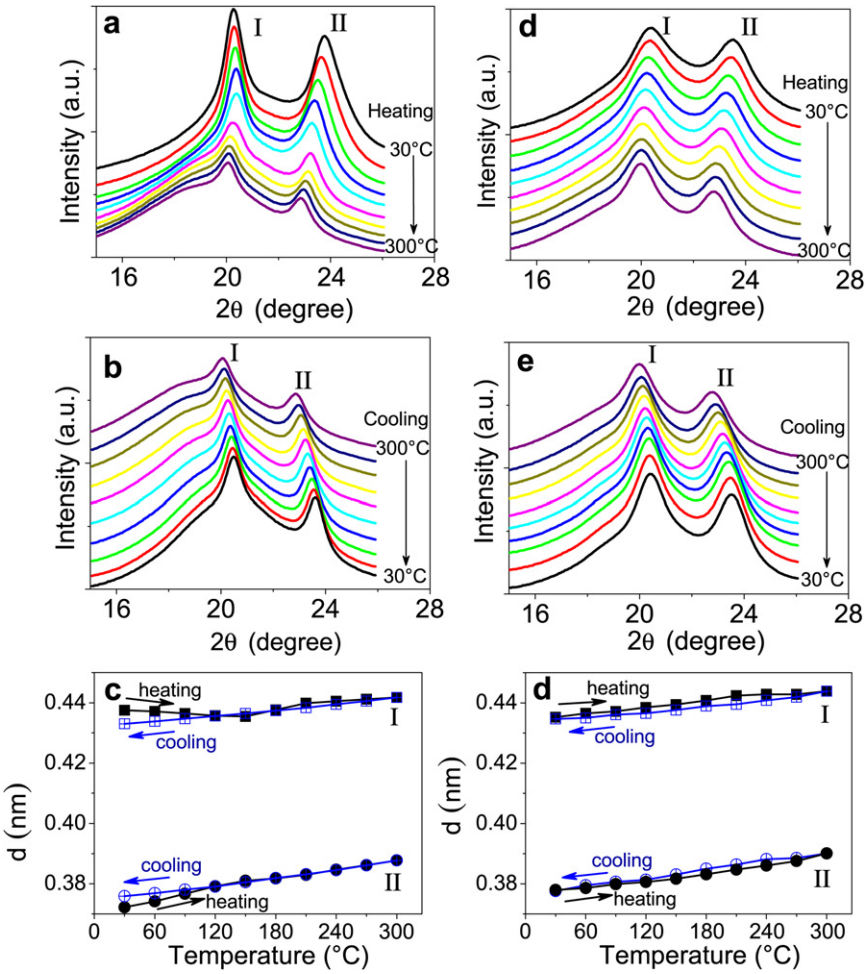

Fig. 3. Behavior of WAXD curves (a, b) and *d*-values (c) of sample T0.15 taken as a function of temperature (30 °C–300 °C–30 °C), behavior of WAXD curves (d, e) and *d*-values (f) of sample T0.6 taken as a function of temperature (30 °C–300 °C–30 °C). All samples were annealed at 180 °C for 2 h before measurements.

behavior can be attributed to the melting process of PA6 blocks and the newly emerged broad peak is consistent with the amorphous peak of pure PA6 [30]. The enhancement of both diffraction peaks during the cooling process is due to the crystallization of PBA and PA6 blocks in the copolymer. While the behavior of sample T0.6 is not the same. As shown in Fig. 3d, e and f, the decrease of peak intensity during the heating process is dimmed and the amorphous peak exists throughout the WAXD measurements.

During the heating process of T0.15 before 150 °C a special peak shift is observed in Fig. 3a. Similar phenomenon has been observed on pure PA6 due to Brill transition, during which the $(200)_\alpha$ and $(002)_\alpha/(202)_\alpha$ diffraction peaks shift to each other and finally turn into γ phase [20,31]. In our experiment, the shift stops before 150 °C and is irreversible during the cooling process (Fig. 3b). The variation of interplanar distances (*d*) during the heating and cooling scan (Fig. 3c) unfolds the above behavior more clearly. However, this behavior is less evident in other samples containing higher volume fraction of PBA, as shown in Fig. 4. The variations of *d*-spacing of samples containing less PA6 (T0.6, T0.5 and T0.4) were almost reversible throughout the temperature scanning. Therefore, this special peak shift in samples containing large ratio of PA6 can be reasonably attributed to the phase transition of PA6 block.

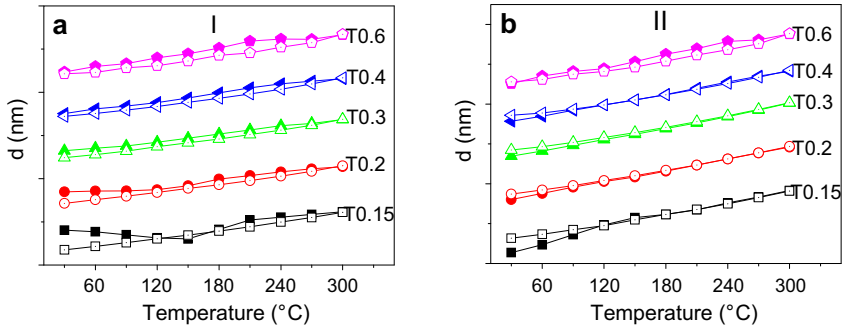

Fig. 4. *D*-spacing (a for peak I, b for peak II) of each sample during heating and cooling scan. The heating and cooling processes are denoted by solid and hollow dot lines, respectively.

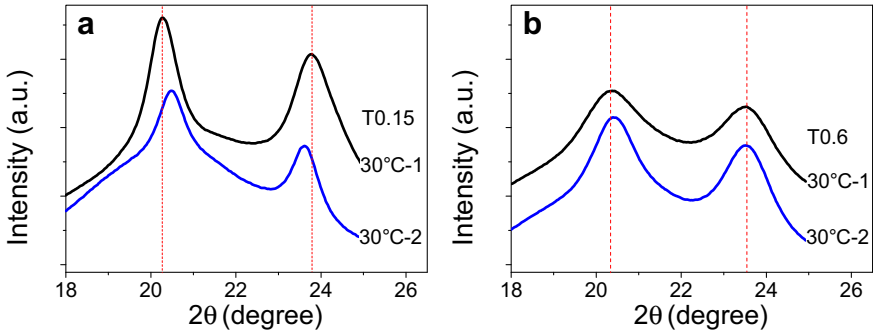

Fig. 5. WAXD curves of T0.15 (a) and T0.6 (b) before (black line) and after (blue line) the heating and cooling scan. Measurements were done at 30 °C. (For interpretation of the references to colour in this figure legend, the reader is referred to the web version of this article.)

A direct comparison of the WAXD curves before and after the heating and cooling scan is presented in Fig. 5, which demonstrates the difference between sample T0.15 and T0.6 more clearly. First, the peak intensity of T0.15 declines significantly after the scan, which is accompanied with the enhancement of the amorphous halo (Fig. 5a). This is due to the irreversible melting of PA6 crystals. On the other hand, the peak intensity of T0.6 elevates due to the crystal perfection of PBA (Fig. 5b). Similar perfection is also expected to occur in T0.15, which may impose strong confinement on PA6 and prevent PA6 from crystallizing during cooling. The peak shift of T0.6 is much less evident than that of T0.15 after the scan. Thus the peak shift in T0.15 can be mainly attributed to the structural change of PA6.

The WAXD peak width increases with the increase of PBA content. Fig. 6 shows the WAXD curves and the corresponding full width at half maximum (FWHM) of all copolymers after the heating and cooling scan. A sharp increase of FWHM with the increase of PBA content of ~45% suggests that the correlation length or perfection of PBA is reduced abruptly.

3.4. FT-IR

To clarify the structure of PA6 block, the annealed samples used in the WAXD measurement were further characterized by FT-IR. Before presenting the FT-IR data, we first verify the internal reference band, which is a basis for quantitative analysis. Fig. 7a displays in situ infrared spectra of sample T0.15 as a function of temperature. The absorption ranging from 2800 to 3000 cm^{-1} represents the stretching vibration of CH_2 (asymmetric and symmetric) whose intensity only has little change with temperature variation (Fig. 7b). Therefore all the other infrared spectra were normalized using the internal reference bands in this rang.

Fig. 7c–f present the FT-IR spectra of all copolymers before and after the programming heating and cooling with a rate of 20 °C/min between 30 and 300 °C. By checking the band assignments of pure PBA and PA6, we picked out the absorption bands which were exclusive to PA6, as shown in Table 3. Previous reports attributed the bands at 1000 cm^{-1} (CO–NH vibration), 1439 cm^{-1} (CH_2 scissors vibration) and 1467 cm^{-1} (CH_2 scissors vibration) to the γ phase of PA6, band at 1199 cm^{-1} (CH_2 twist-wag vibration) to the α phase of PA6, bands at 1430 cm^{-1} (CH_2 scissors vibration), 1460 cm^{-1} (CH_2 scissors vibration) to the mesophase or γ phase. The other bands were still unclear [22]. However, basing on the results of WAXD, there was little γ phase within all samples as the diffraction peaks of γ-form PA6 are not distinguishable from all WAXD curves. Therefore, the bands at 1000, 1439 and 1467 cm^{-1} should be attributed to the quasi-γ mesomorphic order. It seems that the mesomorphic order emerged in our work was quite different from that mentioned early [23]. Furthermore, after heating to 300 °C and programmed cooling (−20 °C/min) to room temperature, the α phase (1199 cm^{-1}) was disappeared and the quasi-γ mesomorphic order retained, as shown in Fig. 7e and f.

For further quantitative analysis about the influence of φ_{PBA} on the morphology of all samples, band at 1000 cm^{-1} was picked out and the Gaussian peak fitting was performed to each of them. Fig. 8 shows the integrated absorbance of 1000 cm^{-1} band from all samples as a function of φ_{PBA}. With the increase of the content of PBA, the integrated absorbance of 1000 cm^{-1} band is increased, which indicates that the stretching effect from PBA favors the formation of the quasi-γ mesomorphic order.

4. Discussion

Based on the above experimental results, it is clear that both PBA and PA6 block were frustrated in the triblock copolymers. In this

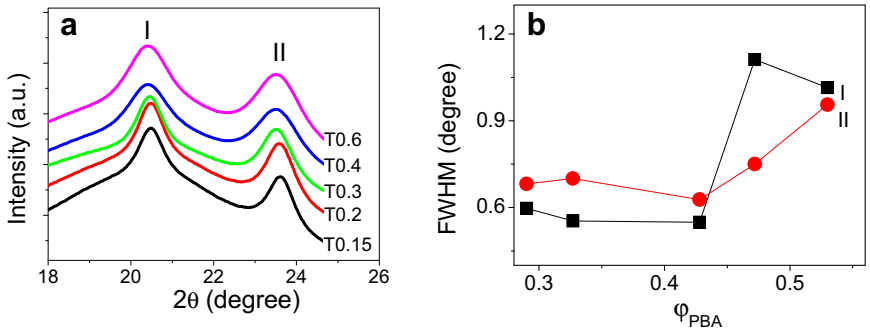

Fig. 6. WAXD curves (a) and the corresponding full width at half maximum (FWHM) (b) of the diffraction peaks of all copolymers after heating and cooling scan. Measurements were done at 30 °C.

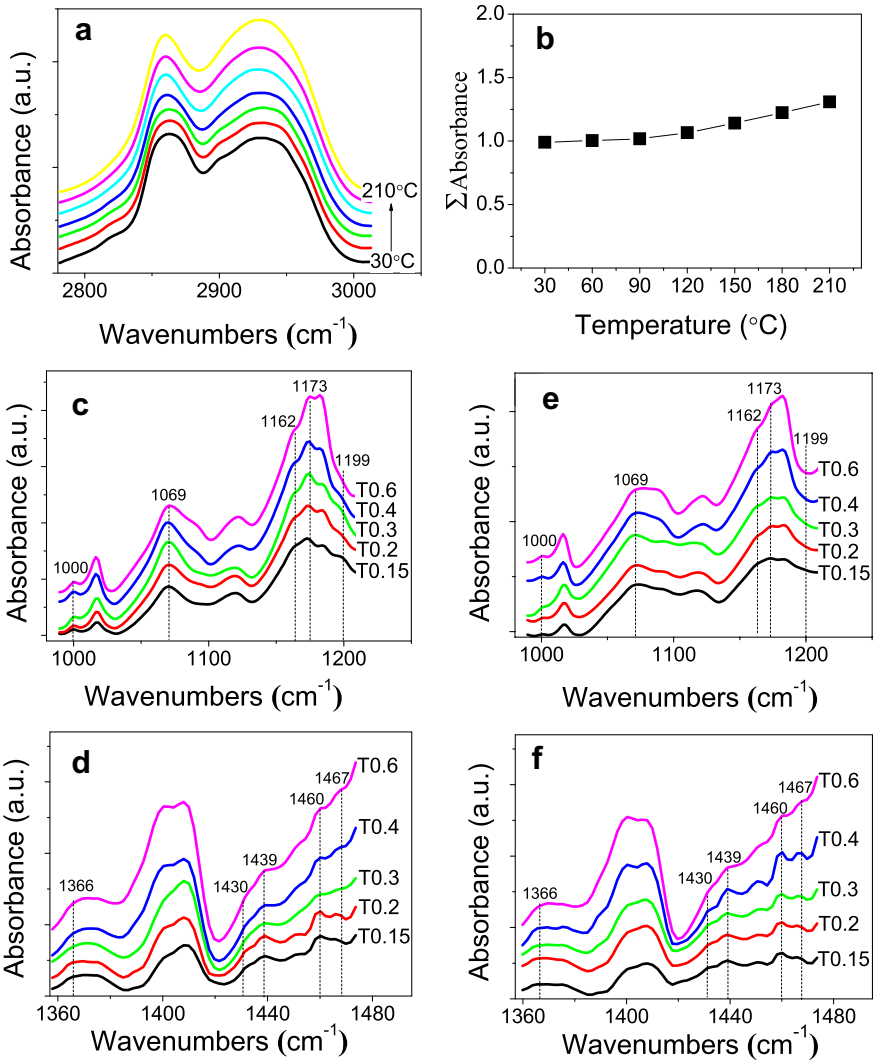

Fig. 7. In situ infrared spectra in the absorption wavenumber range from 2800 to 3000 cm^{-1} of sample T0.15 as a function of temperature (a) and the absorption intensity vs temperature (b). FT-IR spectra of annealed block copolymers at room temperature (c and d), and after heating to 300 °C then programmed cooling (−20 °C/min) (e and f).

section, the following three issues are discussed: (i) what force the PA6 to form mesomorphic order? (ii) what is the state of PA6 block during the heating process? (iii) how does coil-like PA6 hamper the crystallization of PBA?

Fig. 9 compares the crystal structures of PA6 (α, γ) and PBA, where the arrows distinguish between up and down chains, and the dashed lines are traces of sheets of hydrogen bonds [21,25,29]. $S_{PA6(\alpha)}$, $S_{PA6(\gamma)}$ and S_{PBA} represent the calculated cross-section area of each single-chain of them respectively. In our triblock copolymers, the short-chain PA6 ($M_n = 3000$ g/mol) was connected to the rod by amide bonds. The rod-like chains of PBA can easily form close-packed arrays as the intensive π–π interaction and hydrogen bond linkages between each other. Accordingly, in the transition-region of two components, the relative flexible PA6 chains must be forced to pack into parallel fashion. Thus the hydrogen bonds are favorable to form between parallel PA6 chains like that in γ-form crystal [20,21]. To form γ crystal, it requires two anti-parallel hydrogen-bonded sheets as illustrated in Fig. 9b, which however does not exist in the transition-region between two segments in our copolymers. This certainly frustrates the formation of γ-form crystal in the confined PA6 domains. By further analyzing the unit cell structures, we calculated the cross-section area of each single-chain of them, respectively, which leads to a result that $S_{PA6(\alpha)} < S_{PA6(\gamma)} < S_{PBA}$. The cross-section area of PBA is significantly larger than that of PA6 in α form, but relatively closer to that of PA6 chain in γ form. Therefore, there is little chance for PA6 blocks to crystallize near the rod domains, especially in α form. Based on the analysis on the chain alignment and the cross-sections of PBA and PA6 chains in different crystalline forms, it is more prone for PA6 segments near the PBA to form parallelized hydrogen-bonded sheets with a mesomorphic structure close to γ form, which however cannot further develop into three-dimensional crystalline order.

This idea is supported by the WAXD, DSC and FT-IR results. WAXD reveals that no γ-form crystal was formed in all triblock copolymers. From FT-IR measurements, the appearance of bands that previously assigned as γ phase (1000, 1439, 1467 cm^{-1}, Fig. 7)

Table 3
The assignments of infrared absorption bands of PA6 reported previously. In the present paper the bands at 1000, 1439 and 1467 cm^{-1} are attributed to the quasi-γ mesophase of PA6 segments.

Wavenumber (cm^{-1})	1000, 1439, 1467	1199	1430, 1460	1069, 1162, 1173, 1366, 2858, 2929
Assignment	γ	α	Mesophase or γ	Unclear

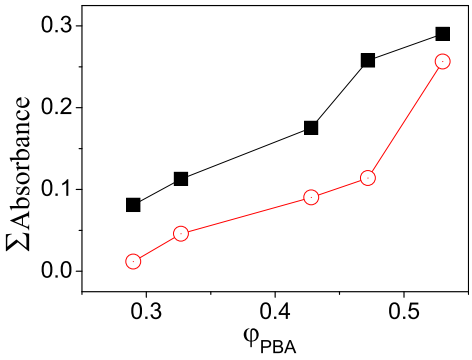

Fig. 8. The plot of the integrated intensity of 1000 cm^{-1} band of all samples vs the content of PBA φ_{PBA}. The line with squares corresponds to Fig. 7c, and the line with circles corresponds to Fig. 7e.

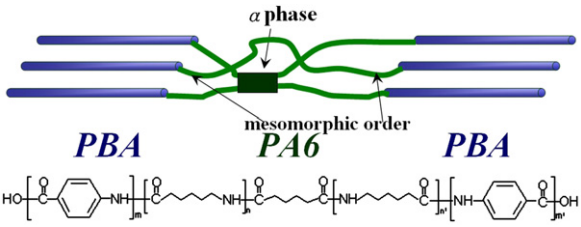

Fig. 10. A schematic model of the organization of the rod–coil–rod block copolymers. The rod-like chains (PBA) tend to form close-packed array. The sandwiched coil segments (PA6) tend to be greatly stretched by the rod segments and stacked in a special way.

conformed the formation of the quasi-γ mesomorphic order. This mesomorphic order is a compromise of the competition between crystallization processes of PA6 and PBA blocks, which shifts to the PBA side with the increase of the content of PBA. Evidently, the content of the mesomorphic order is expected to increase along with the volume fraction of PBA, as supported by the result in Fig. 8. The confinement effect on PA6 segment is also manifested by DSC measurements, where the melting of the crystalline PA6 only appears in samples with low content of PBA (T0.15 and T0.2, see Fig. 2). Similar phenomenon has been reported by de Ruijter et al. in PA6,6/PPTA multi-block copolymer system [33]. Clearly, the confinement frustrates the crystallization process of PA6 and leads to the formation of mesomorphic order, while crystals with small size can form only in the samples with large ratio of PA6.

The behavior of PA6 block during the heating process was observed through WAXD measurement (Fig. 3). As shown in Fig. 9, the $(200)_\alpha$ crystal plane of PA6 which is perpendicular to the *a*-axis was connected by hydrogen bonds. The interplanar distance of $(200)_\alpha$ or the length of hydrogen bond of α-form PA6 reduced during the heating process (Fig. 3), and at 150 °C this behavior stopped. For pure PA6, there is a similar phase transition observed prior to melting and have come to be known as the Brill transition. For Brill transition, the $(200)_\alpha$ and $(002)_\alpha/(202)_\alpha$ diffraction peaks shift to each other and finally turn into a single peak at transition temperature ($T_B \approx 160$ °C for pure PA6) [20,31]. In our copolymers, the γ phase of PA6 has not developed and this special transition ends prematurely as the melt of PA6 segment in the copolymer. In addition, after the melting of PA6, the microdomain of PBA segment reconstructs, and mesomorphic order of PA6 retains. As shown in Fig. 3b, there is little reversion during the cooling process, and α crystal of PA6 does not arise again (Fig. 7e) after programmed cooling (−20 °C/min). Finally, the above behavior only occurs in samples T0.15 and T0.2 which suggests that α crystal of PA6 can form only in the triblock copolymer with low volume fraction of PBA.

Based on the above analysis, a model of this triblock polymer is depicted (Fig. 10), where the PBA blocks are close-packed, and a quasi-γ mesomorphic order of PA6 is nearby the interface between PBA and PA6 domains. With the increase of PA6 content, α crystal of PA6 may form in the middle of the coil domain.

In a rod–coil copolymer system, the stretching effect from rod on the coil is widely recognized [13,34]. In fact the imposed force from rod on the coil equals the counterforce on itself. Normally the interactions between the rods like hydrogen bonding and π–π interaction are much stronger than that between coil segments with van de Waals force. In our system, the counter-stretching from the PA6 block on the rod seems rather strong and does affect the ordering of PBA block, especially in the system with large volume fraction of PBA. The FWHM of WAXD peaks increases with the PBA content, which is partly due to the constraint imposed by PA6 block. With the increase of PBA content, the stretching force between PBA and PA6 blocks increases. This is already demonstrated by the content of quasi-γ mesomorphic order of PA6. In the copolymers we synthesized, both ends of sandwiched PA6 blocks are fixed by rod-like PBA through amide bonds. Therefore, the end-to-end distance of PA6 chain is determined by the length of coil domain after microphase separation. For an ideal chain, the force $\vec{f}$ to hold two ends separated by a vector $\vec{r}$ is linear in $\vec{r}$ according to equation [35]:

$$\vec{f} = \frac{3kT}{R_0^2}\vec{r} \tag{1}$$

where R_0, k and T represent the radius of gyration, Boltzmann constant and absolute temperature, respectively. A rough estimation of the stretching force between the rod and coil is about 5.16×10^{-12} N, which corresponds to a work of 6.59*kT*. This value is about 7% of the melting enthalpy of perfect PA6 crystal [36]. As no

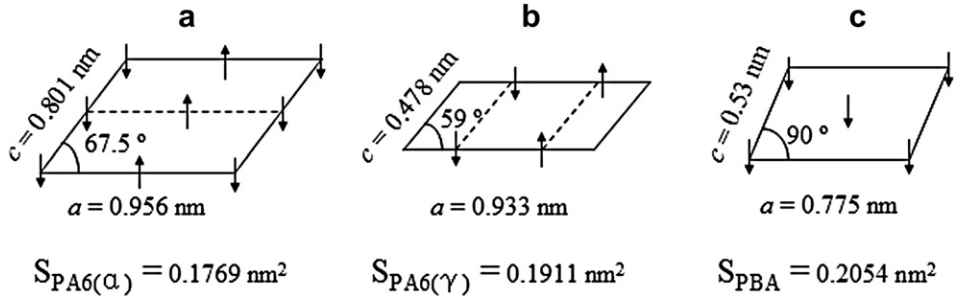

Fig. 9. Crystal structures of PA6 (α, γ) and PBA. The arrows distinguish between up and down chains and the dashed lines are traces of sheets of hydrogen bonds. $S_{PA6(\alpha)}$, $S_{PA6(\gamma)}$ and S_{PBA} represent the calculated cross-section areas of each single-chain in PA6 α, γ and PBA crystal respectively.

melting enthalpy of PBA is available, we cannot make a direct comparison. Nevertheless, the stretching effect due to phase separation is rather large, which is expected to distort the lattice packing of PBA and leads to frustrated structure. This can explain the increase of peak width with the increase of PBA content. The counter-stretching effect from the coil block on the packing of rod is not widely studied, which may need to be considered when designing materials for fiber application.

5. Conclusion

A series of rod–coil–rod triblock copolymers containing rigid PBA and flexible PA6 were synthesized by two-step polycondensation procedures with different block ratios. The frustrated structures of both rod and coil blocks were studied, which is attributed to the stretching effect between each other. For PA6, a novel quasi-γ mesomorphic order is found in the transition-region nearby the PBA domain and is more favored with increasing the content of PBA. The heating behavior of PA6 segments in the copolymers with low volume fraction of PBA shows Brill transition similar with homopolymer PA6, where the length of hydrogen bond between PA6 chains is reduced during the heating process. On the other hand, the crystallization of PBA blocks is also suppressed by PA6 block when the volume fraction of PBA reaches approximately 45%.

Acknowledgment

LBL would like to thank Prof. Stephen Picken for providing chemical compounds and Prof. Wenbing Hu and Dr Yu Ma are acknowledged for the assistance on DSC measurements. This work is supported by the NNSFC (20774091), Fund for one hundred talent scientist, the 'NCET' program and the experimental fund of NSRL.

References

[1] Ruzette AV, Leibler L. Nat Mater 2005;4(1):19–31.
[2] Rabani G, Luftmann H, Kraft A. Polymer 2006;47(12):4251–60.
[3] http://www.dorlastan.com/.
[4] Liu Y, Shao ZZ, Fritz V. Nat Mater 2005;4(12):901–5.
[5] Jin HJ, Kaplan DL. Nature 2003;424(28):1057–61.
[6] König HM, Gorelik T, Kolb U, Kilbinger Andreas FM. J Am Chem Soc 2007;129(3):704–8.
[7] Arun A, Gaymans RJ. Macromol Chem Phys 2008;209(8):854–63.
[8] Lin CL, Tung PH, Chang FC. Polymer 2005;46(22):9304–13.
[9] Leibler L. Macromolecules 1980;13(6):1602–17.
[10] Olsen BD, Segalman RA. Macromolecules 2006;39(20):7078–83.
[11] Pryamitsyn V, Ganesan V. J Chem Phys 2004;120(12):5824–38.
[12] Lee M, Cho BK, Zin WC. Chem Rev 2001;101(12):3869–92.
[13] Liu XB, Zhao YF, Chen EQ, Ye C, Shen ZH, Fan XH, et al. Macromolecules 2008;41(14):5223–9.
[14] Muthukumar M, Ober CK, Thomas EL. Science 1997;277:1225–32.
[15] Tenneti KK, Chen X, Li CY, Tu Y, Wan X, Zhou QF, et al. J Am Chem Soc 2005;127(44):15481–90.
[16] Li LB, Lambreva D, de Jeu WH. J Macromol Sci Phys 2005;43(1):59–70.
[17] De Ruijter C, Jager WF, Groenewold J, Picken SJ. Macromolecules 2006;39(11):3824–9.
[18] De Ruijter C, Mendes E, Boerstoel H, Picken SJ. Polymer 2006;47(26):8517–26.
[19] Matheson Jr RR, Flory PJ. Macromolecules 1981;14(4):954–60.
[20] Murthy NS. J Polym Sci Part B Polym Phys 2006;44(13):1763–82.
[21] Arimoto H, Ishibashi M, Hirai M, Chatani Y. J Polym Sci Part A Gen Pap 1965;3(1):317–26.
[22] Rotter G, Ishida H. J Polym Sci Part B Polym Phys 1992;30(5):489–95.
[23] Auriemma F, Petraccone V, Parravicini L, Corradini P. Macromolecules 1997;30(24):7554–9.
[24] Aharoni SM. N-nylons: their synthesis, structure and properties. New York: John Wiley & Sons Ltd; 1997 (chapter 2.6).
[25] Takahashi Y, Ozaki Y, Takase M, Krigbaum WR. J Polym Sci Part B Polym Phys 1992;31(9):1135–43.
[26] Higashi F, Akiyama N, Ogata S. J Polym Sci Part A Polym Chem 1982;21(3):913–6.
[27] Mark JE. Polymer data handbook. New York: Oxford University Press; 1999.
[28] Bao H, Rybnikar F, Saha P, Yang J, Geil PH. J Macromol Sci Phys 2001;B40(5):869–911.
[29] Rhee S, White JL. Polymer 2002;43(22):5903–14.
[30] Murthy NS, Curran SA, Aharoni SM, Minor H. Macromolecules 1991;24(11):3215–20.
[31] Vasanthan N, Murthy NS, Bray RG. Macromolecules 1998;31(23):8433–5.
[32] Schaefgen JR, Foldi VS, Logullo FM, Good VH, Gulrich LW, Killian FL. Polym Prepr 1976;17:69–74.
[33] De Ruijter C, Jager WF, Li LB, Picken SJ. Macromolecules 2006;39(13):4411–7.
[34] Cavalleri P, Ciferri A, Dell'Erba C, Novi M, Purevsuren B. Macromolecules 1997;30(12):3513–8.
[35] De Gennes PG. Scaling concepts in polymer physics. Ithaca: Cornell University Press; 1979 (part A–I).
[36] Psarski M, Pracella M, Galeski A. Polymer 2000;41(13):4923–32.